Springer

KSME

Journal of Mechanical Science and Technology 24 (7) (2010) 1465~1473
www.springerlink.com/content/1738-494x
DOI 10.1007/s12206-010-0502-5

A numerical prediction on the reduction of microorganisms with UV disinfection †

Chan Li[1], Baoqing Deng[2] and Chang Nyung Kim[1,3,*]

[1]*Department of Mechanical Engineering, Kyunghee University, Yongin 446-701, Korea*
[2]*College of Environment and Architecture, University of Shanghai for Science and Technology, Shanghai 200093, China*
[3]*Industrial Liaison Research Institute, Kyung Hee University, Yongin 446-701, Korea*

(Manuscript Received January 15, 2010; Revised March 31, 2010; Accepted May 6, 2010)

Abstract

This paper investigates the three dimensional flow field and organism concentration in a UV disinfection channel. The modified P-1 model is newly adopted to solve the UV intensity field. This modified P-1 model for radiative transfer can yield an accurate light intensity for even complicated geometries. The effect of UV light intensity on the disinfection of microorganisms has been considered in the species equation. Differently from existing literatures, this study has used the Euler method for the calculation of both the flow field and the concentration of organisms. The CFD modeling results are compared with existing experimental data [1] for a UV channel, which shows outstanding agreement. The effects of inlet velocity, absorption coefficients of lamps quartz and water on the disinfection efficiency are investigated. With a smaller inlet velocity and smaller absorption coefficients, higher disinfection efficiency has been obtained. The current CFD model has the capability to predict the performance of UV disinfection channels.

Keywords: UV disinfection; P-1 model; Computation; Environment; Fluid mechanics; Numerical analysis

1. Introduction

Coliform bacteria are the commonly used bacterial indicator for the sanitation of foods and water. They are abundant in the feces of warm-blooded animals, but can be also found in an aquatic environment, in soil and on vegetation. The existence of coliform bacteria in drinking water may indicate a possible presence of harmful, disease-causing organisms. Some illnesses may be caused by coliform itself in the water. Therefore, coliform bacteria have a significant influence on human health in association with drinking water. Due to their pathogenicity, coliform bacteria have received significant attention. Some methods have been presented to remove coliforms from water, such as chlorination [2], ozonation [3], TiO2 photocatalysis [4] and UV disinfection. Thereinto, the UV disinfection is a widely used method because of its high disinfection efficiency and no secondary pollution. In order to optimize the performance of the UV reactor and to get reliable prediction, a numerical simulation of species transport and disinfection is necessary.

The flow model and disinfection model in water treatment processes have been increasingly developed with the aim of obtaining more reliable predictions and optimizing design parameters. Especially, numerical simulations using computational fluid dynamics (CFD) have been recently paid much attention to. Sozzi and Taghipour [5] investigated the flow field of annular photo-reactor with the Standard k-ε model, the Realizable k-ε model and the Reynolds stress model. Compared with the experimental data, a better consistency has been found in the simulation with the Standard k-ε model than the other two models. The Standard k-ε model was also employed to calculate the flow field by Lyn et al. [6]. Here, good agreement between predictions and measurements has been reported in the results for the velocity, but a striking disparity has been observed for the kinetic energy. Rauen et al. [7] performed the CFD simulations using an improved low-Reynolds number k-ε model to account for relatively low turbulence levels in baffled chlorine contact tanks and good agreement was obtained for the assessed flow features, as characterized from the physical experimentation results.

In the UV disinfection, the distribution of UV intensity is important for the design optimization of the reactor. The radiation transport equation (RTE) can predict the light intensity distribution. Spadoni et al. [8] used a Monte Carlo approach to solve the radiant energy balance equation and to get the distribution of the local rate of energy absorption. A random-walk model developed by Yokota et al. [9] was employed to analyze the light absorption of a photosynthetic microorganism. The discrete ordinate (DO) model was begun to be used to obtain the light intensity distribution a decade year ago [10,

† This paper was recommended for publication in revised form by Associate Editor Haecheon Choi

*Corresponding author. Tel.: +82 31 201 2578, Fax.: +82 31 202 8106
E-mail address: cnkim@khu.ac.kr

11]. The DO model can obtain accurate results because the RTE is calculated by many linear equations for light intensity. However, the DO model makes the calculation complicated and does not conserve the radiant energy at the surfaces of complex geometries especially for the anisotropic scattering [12]. To solve these problems, the P-1 model can be used. In the P-1 model, the RTE is calculated by only one governing equation, which makes the calculation much easier. Also, the P-1 model can solve accurately the light intensity in complex geometries with the anisotropic scattering.

To solve the RTE, the radiation source model is to be decided. Chiu et al. [1] employed the point source method to obtain the intensity field in a whole UV channel. Also, Lyn et al. [6] used the PPS technique with an integral over the length of a UV lamp. A design of a collimator was optimized by use of a numerical model including line source integration (LSI) by Blatchley [13]. On the other hand, the line source model which depicts the lamp as a simple emitting line was used. A conservative variant of the discrete ordinate model was used to solve the RTE by Pareek and Adesina [12]. It can be easily extended to predict light intensity in complex reactor geometries such as parabolic, elliptical, and multiple lamp photoreactors.

There have been many efforts on the inactivation of microorganisms in the UV reactors. Liu et al. [14] simulated the turbulent flow field inside a UV disinfection reactor using some turbulence models, Reynolds stress transport model and two-fluid model. The disinfection was simulated by using the Lagrangian approach. The sensitivity of microorganism inactivation to the turbulence model selection is also investigated. The results showed that the sensitivity increased with increasing UV response kinetics and increased with conditions that promote high log inactivation. The transport of microorganisms can be described by Lagrangian method or Eulerian method. Ducoste [15] used both the Lagrangian and Eulerian methods to model the microbial inactivation. The results showed that the solution obtained by the Eulerian approach seemed comparable to that by the Lagrangian particle tracking approach.

In the above literatures, the obtained turbulent flow fields have not been accurate and the calculated UV intensities have been unreasonable because of the use of the simple model of light distribution, which has resulted in underestimate or overestimate of the disinfection efficiency. However, the actual arrangement of the UV lamps may be complicated so that the DO model and Lagrangian method may not be feasible to get accurate UV intensity fields.

In the present study, the low-Re number k-ε turbulence model has been used to calculate the flow field. The P-1 model for radiative transfer has been used to solve the UV intensity field, which can account for complicated geometries. The species equation based on the Euler method has been applied to predict the concentration of organisms in conjunction with the inactivation effect caused by UV light. The numerical results have been compared with existing experimental measurements [1] in a laboratory-scale UV reactor and the effect of inlet velocity and absorption coefficients of lamp quartz and water on disinfection efficiency has been investigated.

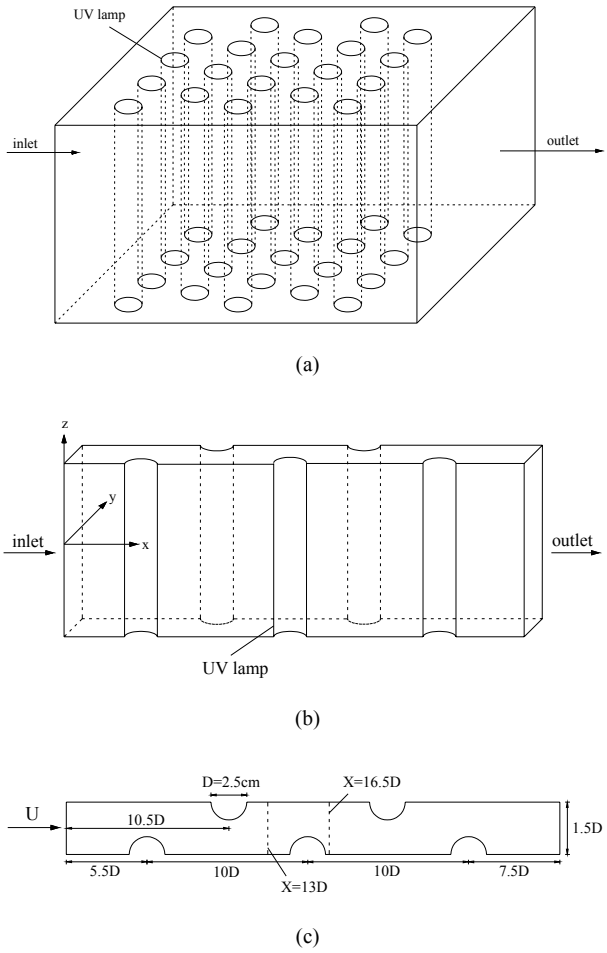

Fig. 1. Geometrical configuration of UV reactor (a) whole geometry (b) modeled central region (c) plane view of the modeled region (not in scale).

2. Problem formulation and numerical simulation setup

2.1 Geometry of the reactor

The physical model of the reactor is 0.33 m wide, 0.825 m long and 0.76 m deep as shown in Fig. 1(a). The UV lamps (diameter D is 2.5 cm) are arranged in four rows, with five lamps in each row, in a staggered configuration. The flow passes through the UV channel at different inlet velocities.

To keep high spatial resolution at reasonable computational effort, only a central region rather than the entire flow region is considered. The modeled region is 33D long, 1.5D wide and 30.4D deep (Fig. 1(b)). The first lamp is 5.5D away from the entrance, and the locations of the lamps are shown in Fig. 1(c). Since the UV disinfection can be expected in the flow domain, the current numerical analysis has been carried out only for the flow domain.

2.2 Flow modeling

The flow in the UV reactor has a strong influence on the distribution and disinfection of microorganisms. Therefore, it is necessary to predict the flow field in the UV channel accurately. The flow in the reactor can be described by the continuity and three-dimensional Navies-Stokes equations. Based on the eddy-viscosity approximation, the governing equations can be written as follows.

$$\frac{\partial}{\partial x_j}\left(\rho u_j\right)=0 \tag{1}$$

$$\frac{\partial}{\partial x_j}\left(\rho u_i u_j\right)=-\frac{\partial p}{\partial x_i}+\frac{\partial}{\partial x_j}\left[\rho\left(\nu+\nu_t\right)\frac{\partial u_i}{\partial x_j}\right]+\rho g_i \tag{2}$$

$$\nu_t=C_\mu f_\mu \frac{k^2}{\varepsilon} \tag{3}$$

where ν and ν_t are the laminar and turbulent kinematic viscosities of the water, respectively. The latter one should be determined by a suitable turbulence model. In the present study, the low-Re number k-ε turbulence model is used to determine the turbulent kinematic viscosity. The governing equations of the turbulent kinetic energy k and its dissipation rate ε are written as follows:

$$\frac{\partial}{\partial x_j}\left(\rho u_j k\right)=\frac{\partial}{\partial x_j}\left[\rho\left(\nu+\nu_t/\sigma_k\right)\frac{\partial k}{\partial x_j}\right]+G_k-\rho\varepsilon \tag{4}$$

$$\frac{\partial}{\partial x_j}\left(\rho u_j \varepsilon\right)=\frac{\partial}{\partial x_j}\left[\rho\left(\nu+\nu_t/\sigma_\varepsilon\right)\frac{\partial \varepsilon}{\partial x_j}\right]+C_{\varepsilon 1}\frac{\varepsilon}{k}G_k-C_{\varepsilon 2}f_\varepsilon\rho\frac{\varepsilon^2}{k} \tag{5}$$

$$f_\varepsilon=\left\{1-\exp\left[-\frac{y^*}{3.1}\right]\right\}^2\times\left\{1-0.3\exp\left[-\left(\frac{R_t}{6.5}\right)^2\right]\right\} \tag{6}$$

where the model constants are given by Abe et al. [16] as follows:

$$C_\mu=0.09,\quad \sigma_k=1.4,\quad \sigma_\varepsilon=1.4\ \ C_{\varepsilon 1}=1.5,\quad C_{\varepsilon 2}=1.9$$

The flow equations must be complemented by boundary conditions. At the inlet, five different uniform unidirectional velocities (U = 0.09, 0.12, 0.15, 0.18 and 0.21 m/s) are considered. Turbulent intensity is set to be $0.16\mathrm{Re}^{-1/8}$ and turbulent length scale is 2.5 cm. At all walls, no-slip boundary condition is used for velocity and turbulence, respectively. On the lateral boundaries (excepting the solid boundaries), a symmetry condition is imposed, so that there is no flux across them.

2.3 Radiation model

The radiation transport equation for an absorbing, emitting and scattering medium at position $\vec{r}$ in the direction $\vec{s}$ can be written in the following equation [17].

$$\frac{dI(\vec{r},\vec{s})}{ds}=-aI(\vec{r},\vec{s})-\sigma_s I(\vec{r},\vec{s})+\frac{\sigma_s}{4\pi}\int_{4\pi} I(\vec{r},\vec{s}')\Phi(\vec{s},\vec{s}')d\Omega' \tag{7}$$

where I is light intensity ($\mathrm{W\text{-}m^{-2}\text{-}sr^{-1}}$), a is the absorption coefficient ($\mathrm{m^{-1}}$), and σ_s is the scattering coefficient ($\mathrm{m^{-1}}$). The first term on the right-hand side represents the loss of photons resulting from absorption, the second term means the loss of radiation attributed to out-scattering, and the last term accounts for the gain in the radiation attributed to in-scattering, where $\Phi(\vec{s},\vec{s}')$ is the phase function for the in-scattering of photons.

In this paper, the P-1 model with appropriate boundary conditions is used to solve the radiative transport equation and to evaluate the light intensity distribution in the flow domain of a UV channel. In the P-1 method, the radiation intensity is expanded in terms of its moments in the following equations [18].

$$I(\vec{r},\vec{s})=\frac{1}{4\pi}\left[G(\vec{r})+3\vec{s}\cdot\vec{q}(\vec{r})\right] \tag{8}$$

with

$$G(\vec{r})=\int_{4\pi} I(\vec{r},\vec{s})d\Omega \tag{9}$$

$$\vec{q}(\vec{r})=\int_{4\pi} I(\vec{r},\vec{s})\vec{s}d\Omega \tag{10}$$

where $G(\vec{r})$ is the incident radiation ($\mathrm{W\text{-}m^{-2}}$) and $\vec{q}(\vec{r})$ is the radiation heat flux ($\mathrm{W\text{-}m^{-2}}$). Since the incident radiation G is the integration of light intensity with respect to the direction, it is independent of the direction.

The transport equation for the incident radiation G ($\mathrm{W\text{-}m^{-2}}$) is shown as follows [17].

$$\nabla\cdot(\Gamma\nabla G)-aG=0 \tag{11}$$

$$\vec{q}(\vec{r})=-\Gamma\nabla G \tag{12}$$

with

$$\Gamma=\frac{1}{3(a+\sigma_s)-C_1\sigma_s} \tag{13}$$

where Γ is the diffusion coefficient of G; C_1 is the linear-anisotropic phase function coefficient.

Thus, the incident radiation can be obtained easily by solving the simple diffusion equation, i.e., Eq. (11), instead of the complicated integro-differential equation, i.e., Eq. (7).

The boundary condition to be used with the P-1 model can be obtained as follows [17].

$$-\Gamma_G \frac{\partial G}{\partial n} = -\frac{4G_0 - (1-\rho_w)G}{2(1+\rho_w)} \tag{14}$$

where ρ_w means the wall reflectivity.

To solve the intensity field of the UV disinfection channel, the irradation coming from the outside of the computational domain (that is, the outer surface of quartz tube) are required. The value of irradiation G_0 at the outer surface of UV lamp can be obtained as follows [17].

$$G_0(r=R,z) = \frac{S}{L}\int_{-L/2}^{L/2} \frac{1}{4\pi\left(R^2+(z-h)^2\right)} \exp\left[-\alpha_q (t/R)\sqrt{R^2+(z-h)^2}\right] dh \tag{15}$$

where S is the lamp output power (26.7 W); L is the length of the lamp (0.76 m); r is the radial distance between a point in the flow domain (r,z) and the center of a single lamp centered ($0,z$) (m); z is the vertical coordinate (m); R is the radius of the tube (1.25×10^{-2} m); α_q is the absorption coefficient of radiation in quartz tube (63 m^{-1}) [1]; t is the thickness of the quartz tube (1.5×10^{-3} m).

For the inlet and outlet of the reactor, the emissivity is taken to be unity, meaning no reflection. Since there is no irradiation from the top and bottom walls, G_0 is taken to be zero.

2.4 Species equation

Through the irradiation of the UV light, the DNA or RNA structure of microorganisms can be destroyed. The inactivation kinetics can be included in the species equation, which can be given as follows.

$$\frac{\partial}{\partial x_j}\left(\rho u_j C\right) = \frac{\partial}{\partial x_j}\left[\rho\left(\frac{\nu}{Sc}+\frac{\nu_t}{\sigma_c}\right)\frac{\partial C}{\partial x_j}\right] + \rho S \tag{16}$$

$$S = -KGC \tag{17}$$

where C is the organism concentration (Kg-m^{-3}); K is an intrinsic rate constant with a value of 0.059 m^2-W^{-1}-s^{-1} [1].

2.5 Numerical procedure

The finite-volume method is adopted to solve three-dimensional governing equations. A commercial software FLUENT 6.3 is used to solve the continuity, momentum, turbulence and species equations. The second-order upwind scheme is used to discretize the convective terms and the central difference scheme for diffusion terms. The SIMPLE algorithm is used for velocity-pressure coupling. The convergence criterion is 10^{-4} for continuity, momentum and turbulence and 10^{-6} for light intensity and concentration.

3. Results and discussion

An experimental study in the UV disinfection channel was carried by Chiu et al. [1]. The UV reactor was 0.92 m deep, 0.33 m wide, and 3 m long. Two modules of 20 lamps each (76 cm arc length and 2.5 cm diameter) was placed in series in the middle region of the channel. Lamps were arranged in four rows, each row has five lamps, with a staggered configuration. The lamp spacing was 12.5 cm between each row and 7.5 cm between adjacent tubes in a row. Only one module was illuminated during the pilot experiments. The inlet velocity was ranging from 0.07 to 0.22 m/s, corresponding to Reynolds numbers of 1,750-5,500.

Employing the geometric configurations and flow velocity used in the experimental test, this paper, using the numerical method described in Chapter 2, will examine the flow field and disinfection characteristics of the reactor given in the experiment. The comparisons between simulation results and experimental data will be given.

3.1 Grid independence

In order to ensure grid independence of the numerical results, a comprehensive grid sensitivity study is performed. The simulations for grid sensitivity analysis are conducted for two grid systems of 641,610 grids and 805,077 grids. In each simulation, finer grid is set near the UV lamps to account for the analysis of detailed flow pattern. The results are compared in terms of the calculation time and the velocity along a line in the mid plane of the UV reactor. For N = 641,610, it takes around 8 hours to get convergence, while for N = 805,077, it costs around 20 hours. The comparison of the mean streamwise velocities u/U along the line $y/D = 0$ obtained by the two grid systems is shown in Fig. 2, which reveals outstanding agreement between the results of the two grid systems.

The most limiting factor in performing three dimensional CFD simulations for real engineering problem is the grid number, which directly controls the overall cost of the simulation. On the basis of this grid sensitivity analysis, the grid

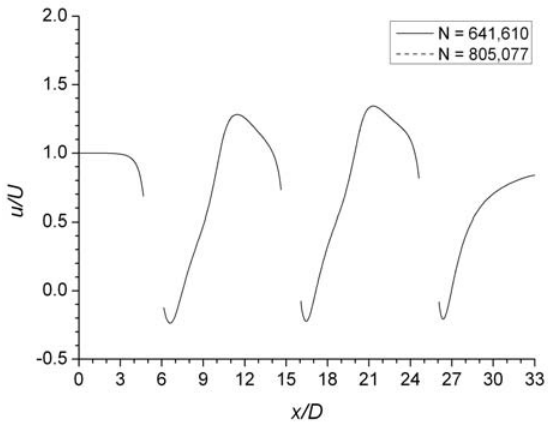

Fig. 2. Comparison of the mean streamwise velocities along the line of $y/D = 0$ for two different grid systems.

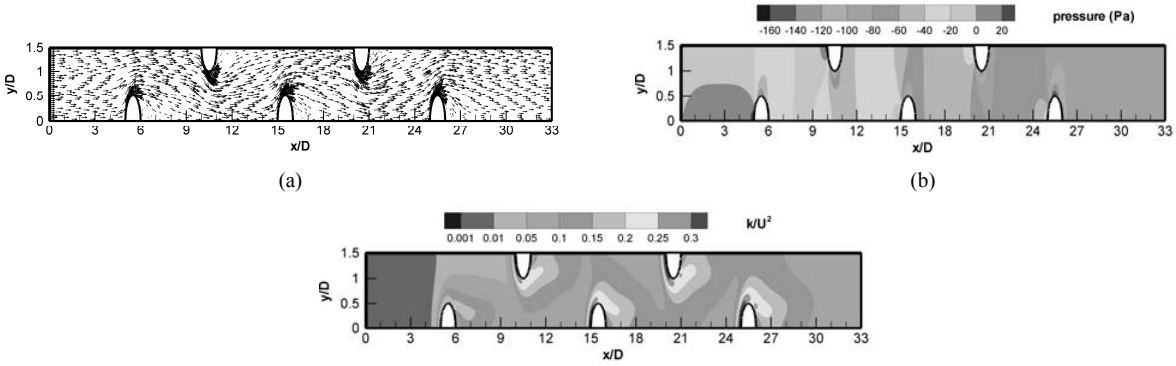

(a) (b)

(c)

Fig. 3. The flow field in the mid plane of the UV reactor (a) plot of velocity vector (b) contour of pressure (c) contour of turbulent kinetic energy.

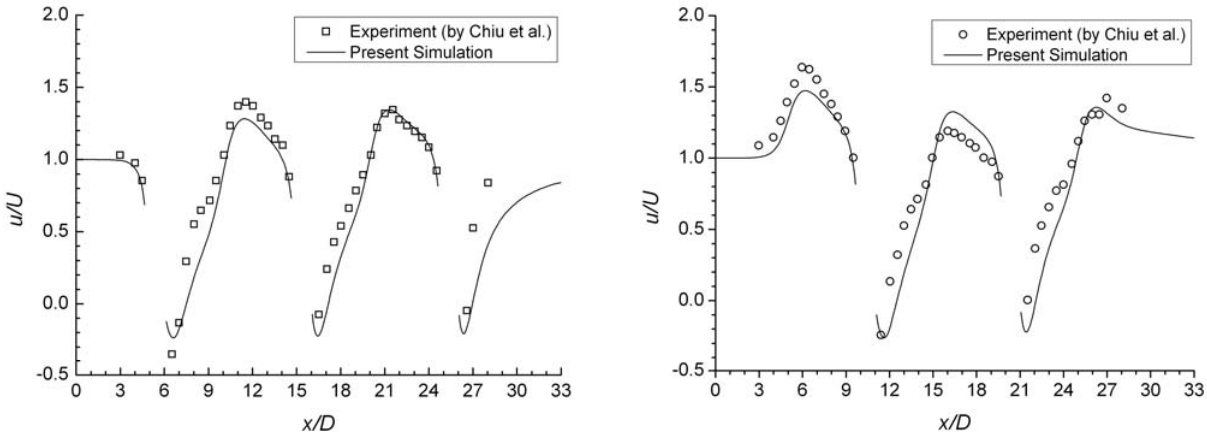

(a) $y/D = 0$ (b) $y/D = 1.5$

Fig. 4. The mean streamwise velocities along two lines (a) $y/D = 0$ (b) $y/D = 1.5$.

number is set to be 641,610 for the current numerical simulations so as to reduce the required computing time.

3.2 Results of flow field

The finite-volume method Fig. 3(a) gives the plot of velocity vector in the mid plane, where wavy velocity pattern for the main stream of the water is observed with a recirculation region in the rear of each lamp. The contours of pressure and turbulent kinetic energy are shown in Fig. 3(b) and (c). The pressure, in general, decreases as the water flows to the downstream. It can be seen that near the frontal surface of the lamp (facing the flow moving to the right), the pressure is higher while near the rear surface of the lamp, the pressure is rather smaller with the smallest pressure near the top or bottom of a lamp. The turbulent kinetic energy in the inlet and outlet region is lower than that in the regions around the UV devices. The largest turbulent kinetic energy is found in the front side of each UV lamp.

The mean streamwise velocities u/U along the lines $y/D = 0$ and $y/D = 1.5$ are shown in Fig. 4. Because the two sections $y/D = 0$ and $y/D = 1.5$ pass through the centre of UV lamps, the gaps of the segments of the curves are caused by the presence of the lamps. At the upstream section of each UV lamp, the streamwise velocity u/U decreases along x direction. The values of u/U after each lamp are negative which means the direction of velocity is opposite, because the reverse flow in the recirculating flow region is generated in these regions.

The mean transverse velocities v/U along the lines $y/D = 0.5$ and $y/D = 1.0$ are depicted in Fig. 5. When the fluid approaches the lamps, the values of v/U increase rapidly because of the presence of the lamps. Near the wake formed after the lamp, the value decreases to be negative in association with the effect caused by the flow around lamps in the opposite row of the UV reactor. For u/U and v/U, good agreement between predictions and measurements is observed with some disparity. Two cross sections ($x/D = 13$ and $x/D = 16.5$) located between two successive lamps are chosen, with the latter including a recirculation region. The comparison of the mean streamwise velocities u/U along the two cross sections obtained by the simulation and experiment are shown in Fig. 6. The predictions of u/U are rather good. In some sections the mean streamwise velocities are small, because of the geometrical closeness to the UV lamps. In Fig. 6(b), the negative value of

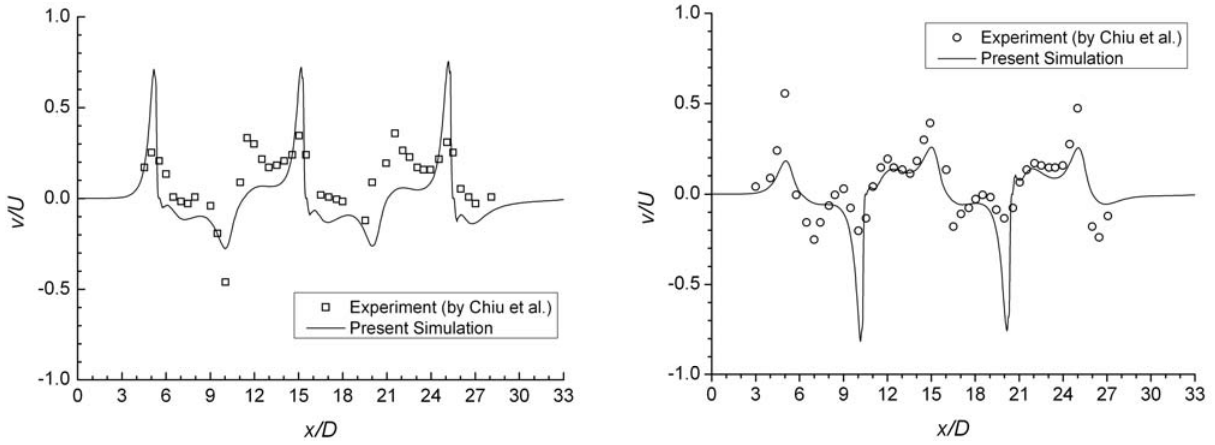

(a) $y/D = 0.5$ (b) $y/D = 1.0$

Fig. 5. The longitudinal profile of mean transverse velocities along two lines (a) $y/D = 0.5$ (b) $y/D = 1.0$.

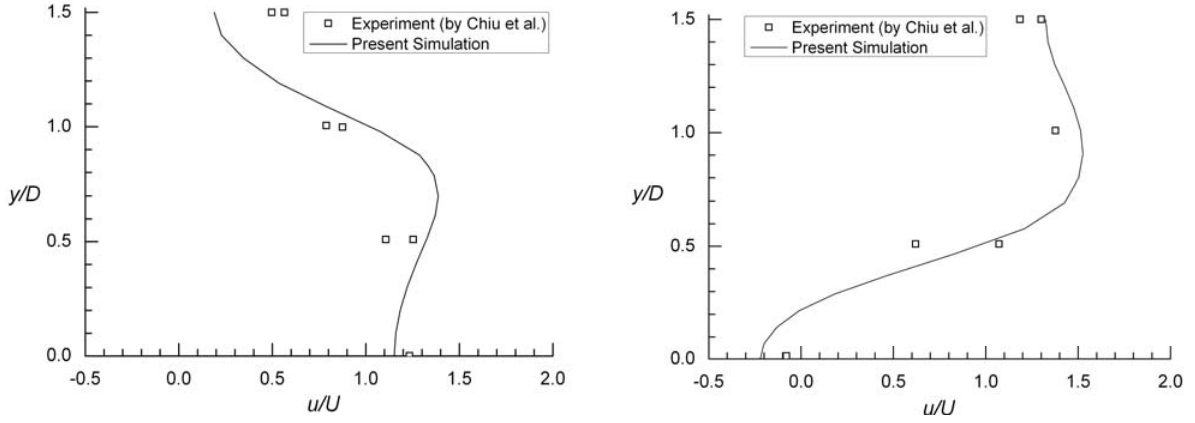

(a) $x/D = 13$ (b) $x/D = 16.5$

Fig. 6. Comparison of the mean streamwise velocities between the low-Re number model and experimental results along two lines (a) $x/D = 13$ (b) $x/D = 16.5$.

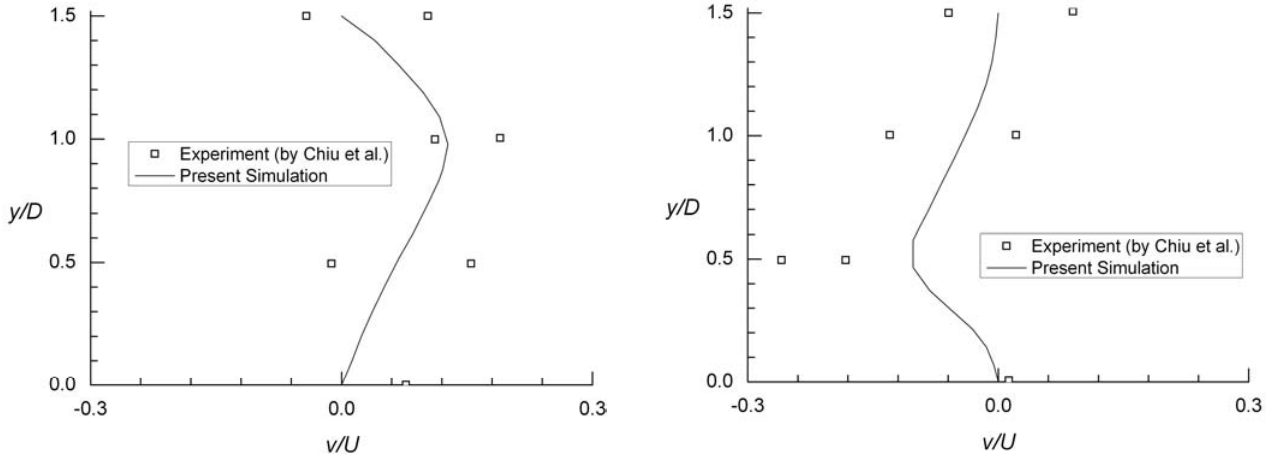

(a) $x/D = 13$ (b) $x/D = 16.5$

Fig. 7. Comparison of the mean transverse velocities between the low-Re number model and experimental results along two lines (a) $x/D = 13$ (b) $x/D = 16.5$.

u/U is seen between *y/D* = 0 to *y/D* = 0.25, because the reverse flow is generated in the recirculation region.

The comparison of the mean transverse velocities obtained by the simulation and experiment at the two *x/D* sections are given in Fig. 7. Although the measured *v/U* profiles exhibit large scatter, the numerical results are often within the scatter of the measurements. In Fig. 7(a), since the cross section *x/D* = 13 is located in the middle of two successive lamps (the front one is in higher *y/D* position and the rear one is in lower y/D position), the fluid flows upward between the two lamps. So the mean transverse velocities are positive in association with the positions of the two lamps. Similar reason can be given on the negative velocities shown in Fig. 7(b).

3.3 Results of disinfection simulation

The UV light intensity distribution on the surface of a UV lamp is illustrated in Fig. 8(a). Since the line source method is employed to evaluate the light intensity, the light intensity in the centre of the lamp is larger than that at the two edges. The intensity field in the mid plane of the UV channel is depicted in Fig. 8(b). The light intensity near the quartz tube of a lamp is very high, while the intensity in a place between two adjacent lamps is very low.

Fig. 9 depicts the microorganism concentration in the mid plane of the UV disinfection channel when the inlet velocity is 0.15 m/s. The concentration of microorganisms is small in theregion just behind the UV lamp, because the fluid stays in a recirculation region for a long time. As the fluid passes the light emitted from quartz tubes, the concentration decreases along x direction.

One of the most important parameter for the disinfection channel is the disinfection efficiency which is defined by the logarithmic ratio of the difference in the microorganism con centration at the inlet and outlet to the concentration at the inlet, which can be written as $\log10\{(C_0 - C_{out})/C_0\}$. In Fig. 10, the disinfection efficiencies for the three dimensional geometry and for the mid-plane of the reactor are compared with those of experimental data obtained by Chiu et al. [1]. It can be seen that the two types of numerical results fall in the mid-area of scattered experimental data. The mid-plane result is somewhat higher than the three-dimensional results, which is caused by the fact that the light intensity in the mid-plane is a little bit higher than the averaged light intensity in the whole reactor. Here, as the inlet velocity increases, the disinfection efficiency decreases. This is because the retention time decreases with the increase of the inlet velocity. Then, the Organisms have little opportunity to absorb UV light.

Total disinfection rate of microorganisms $(C_0 - C_{out})Q$ in the reactor can be considered where Q is the volume flow rate of the water in the reactor. In Fig. 11, it is seen that as the inlet velocity increases, the total disinfection rate increases since more microorganisms are under reaction. Outstanding agreement is seen between the measured and predicted results. Based on the simulation results, an empirical relationship be-

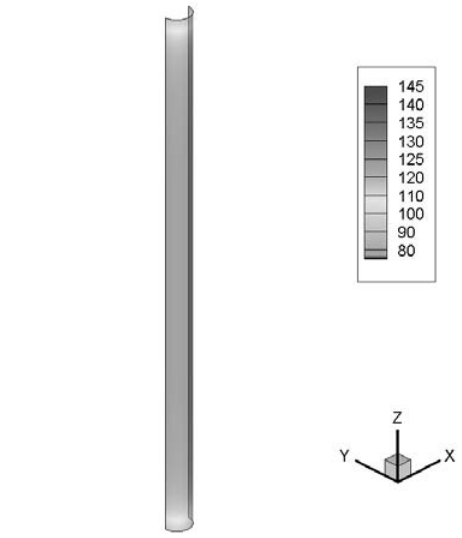

(a)

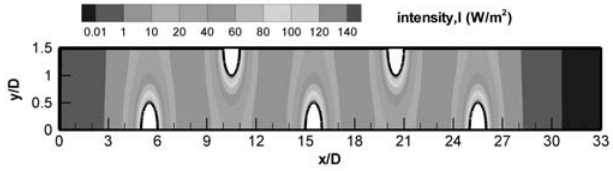

(b)

Fig. 8. The light intensity distribution (a) on the surface of lamp (b) in the centre section of lamp (not in scale).

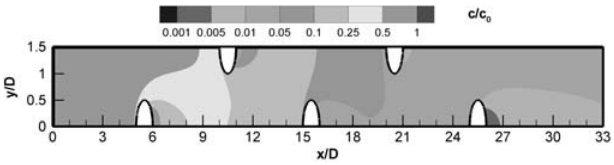

Fig. 9. The concentration field of the disinfection channel at the inlet velocity U = 0.15 m/s (not in scale).

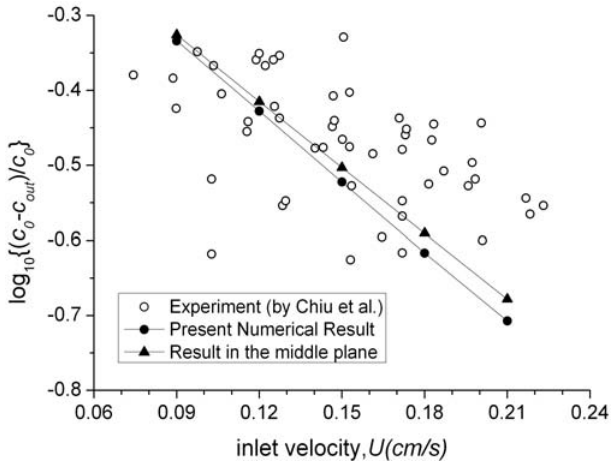

Fig. 10. Comparison of measured and predicted logarithmic disinfection efficiency $\log10\{(c_0-c_{out}/c_0)\}$ as function of inlet velocity.

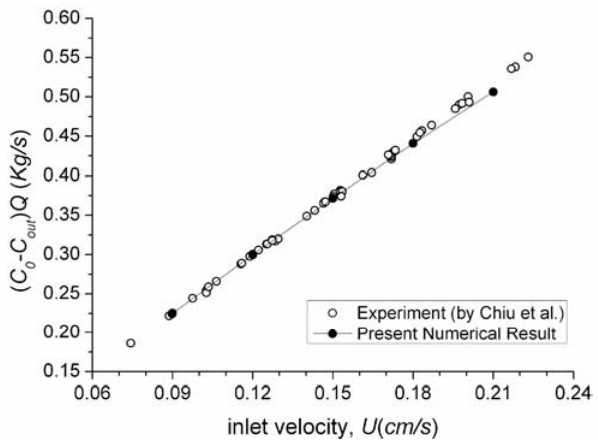

Fig. 11. Comparison of measured and predicted total disinfection rates of microorganisms $(c_0-c_{out})Q$, as function of inlet velocity.

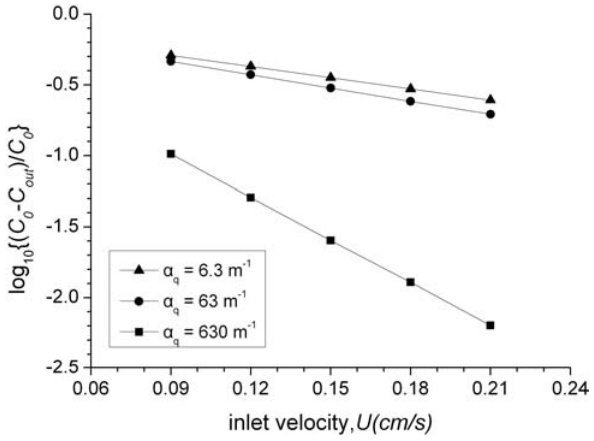

Fig. 12. The effect of absorption coefficient in lamp material on disinfection efficiency $\alpha_w = 43$ m^{-1}.

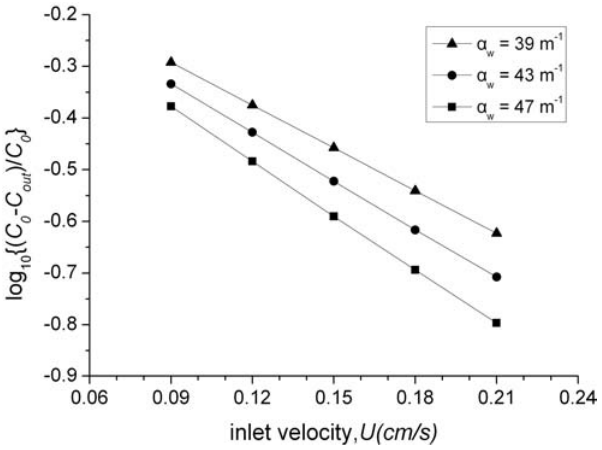

Fig. 13. The effect of absorption coefficient in water on disinfection efficiency with $\alpha_q = 63$ m^{-1}.

tween the total disinfection rate and the inlet velocity can be fitted as $(C_0 - C_{out})Q = aU + b$, where a and b are constants to be found with the linear regression of the simulation results. The values of a and b can be obtained to be 2.341 Kg/m and 0.017 Kg/s, respectively.

As shown in Eq. (15), the adsorption coefficient of radiation in quartz tube αq is a significant parameter for light intensity on the outer surface of the UV lamp. Different tubing materials may lead to different values of absorption coefficient αq. Three different values of absorption coefficient α_q (6.3 m^{-1}, 63 m^{-1} and 630 m^{-1}) are considered in this paper. Thereinto, the value of 63 m^{-1} is from the paper written by Chiu et al. [1], and the other two values are chosen for examining the effects of α_q on the disinfection efficiency. The effect of absorption coefficient α_q on the disinfection efficiency with the absorption coefficient of water $\alpha_w = 43$ m^{-1} is illustrated in Fig. 12. Clearly, as the absorption coefficient α_q increases, the disinfection efficiency decreases. That is because with larger α_q more light has been absorbed by the lamp materials so that the light intensity on the outer surface of the lamp reduces. Obviously, it leads to the fact that the light intensity in the flow domain decreases too. Also, as shown in Fig. 12, the disinfection efficiency is small when α_q is large (say, $\alpha_q = 630$ m^{-1}). Therefore, to get higher disinfection efficiency, the tubing material with lower α_q should be used.

For the P-1 model, the transfer of radiation has some relationship with the absorption coefficient of radiation in water α_w as shown in Eq. (11) and (13). If the concentrations or types of contaminant in the water are different, the absorption coefficients α_w are also different. Three values of α_w (39 m^{-1}, 43 m^{-1} and 47 m^{-1}) are introduced here. Thereinto, the value of 43 m^{-1} is the absorption coefficient in water used by Chiu et al. [1], and the other two values are considered to investigate the effects of α_w on the disinfection efficiency. Fig. 13 illustrates the effect of absorption coefficient α_w on the disinfection efficiency with $\alpha_q = 63$ m-1. The disinfection efficiency decreases as the absorption coefficient α_w increases. That is to say that more light has been absorbed in the vicinity of the UV lamp with the increase in the absorption coefficient α_w.

4. Conclusion

This paper numerically investigates the effect of UV disinfection on the organism concentration in a UV disinfection channel where vertical ultraviolet lamps are arranged in a staggered configuration. This study consists of modeling the flow field and microorganism concentration using the Euler method. The P-1 model for radiative transfer equation has been applied to solve the light intensity in a UV disinfection channel. A commercial software FLUENT 6.3 has been employed to solve the continuity, momentum and species equations and a grid sensitivity analysis has been performed in order to ensure grid independency of the current numerical results. It is shown that the pressure and turbulent kinetic energy are larger in the front side of each UV lamp than in other area and that a recirculation region and low microorganism concentration are found in the rear of each lamp. The disinfection efficiency changes significantly with a change of inlet velocity, the absorption coefficients of tube quartz and water.

With a smaller inlet velocity and smaller absorption coefficients, higher disinfection efficiency has been obtained. The current CFD modeling results are in good agreement with existing experimental data for the UV disinfection channel. This study shows that the present CFD model is capable of predicting the performance of UV disinfection channels.

Acknowledgment

This research was supported partly by the Basic Science Research Program through the National Research Foundation of Korea (NRF) funded by the Ministry of Education, Science and Technology (No. 2009-0063383), and partly by Innovation Program of Shanghai Municipal Education Commission (10YZ95).

References

[1] K. Chiu, D. A. Lyn, P. Savoye and E. R. Blatchley, Integrated UV Disinfection Model Based on Particle Tracking, *J. Environ. Eng-ASEC*. 125 (1) (1999) 7-16.

[2] H. M. Murphy, S. J. Payne and G. A. Gagnon, Sequential UV-and chlorine-based disinfection to mitigate Escherichia coli in drinking water biofilms, *Water. Res*. 42 (2008) 2083-2092.

[3] P. Paraskeva and N. J. D. Graham, Treatment of a secondary municipal effluent by ozone, UV and microfiltration: microbial reduction and effect on effluent quality, *Desalination* 186 (2005) 47-56.

[4] L. Rizzo, Inactivation and injury of total coliform bacteria after primary disinfection of drinking water by TiO_2 photocatalysis, *J. Hazard. Mater*. 165 (2009) 48-51.

[5] D. A. Sozzi and F. Taghipour, Computational and experimental study of annular photo-reactor hydrodynamics, *Int. J. Heat. Fluid. Fl*. 27 (2006) 1043-1053.

[6] D. A. Lyn, K. Chiu and E. R. Blatchley, Numerical Modeling of Flow and Disinfection in UV Disinfection Channels, *J. Environ. Eng*. 125 (1) (1999) 17-26.

[7] W. B. Rauen, B. Lin, R. A. Falconer and E. C. Teixeira, CFD and experimental model studies for water disinfection tanks with low Reynolds number flows, *Chem. Eng. J*. 137 (2008) 550-560.

[8] G. Spadoni, E. Bandini and F. Santarelli, Scattering Effects in Photosensitized Reactions, *Chem. Eng. Sci*. 33 (1978) 517-524.

[9] T. Yokota, K. Yashima, T. Takigawa and K. Takahashi, A New Random-Walk Model for Assessment of Light Energy Absorption by a Photosynthetic Microorganism, *J. Chem. Eng. JPN*. 24 (1991) 558-562.

[10] R. L. Romero, O. M. Alfano and A. E. Cassano, Cylindrical Photocatalytic Reactors. Radiation Absorption and Scattering Effects Produced by Suspended Fine Particles in an Annular Space, *Ind. Eng. Chem. Res*. 36 (8) (1997) 3094-3109.

[11] G. Sgalari, G. Camera-Roda and F. Santarelli, Discrete Ordinate Method in the Analysis of Radiative Transfer in Photocatalytically Reacting Media, *Int. commun. Heat. Mass*. 25 (5) (1998) 651-660.

[12] V. K. Pareek and A. A. Adesina, Light intensity distribution in a photocatalytic reactor using finite volume, *AIChE*. 50 (6) (2004) 1273-1288.

[13] E. R. Blatchley, Numerical modelling of UV intensity: Application to collimated-beam reactors and continuous-flow systems, *Water. Res*. 31 (9) (1997) 2205-2218.

[14] D. Liu, W. Chin, K. linden and J. Ducoste, Numerical simulation of UV disinfection reactors: Evaluation of alternative turbulence models, *Appl. Math. Model*. 31 (2007) 1753-1769.

[15] J. J. Ducoste, D. Liu and K. Linden, Alternative Approaches to Modeling Fluence Distribution and Microbial Inactivation in Ultraviolet Reactors: Lagrangian versus Eulerian, *J. Environ. Eng*. 131 (10) (2005) 1393-1403.

[16] K. Abe, T. Kondoh and Y. Nagano, A new turbulence model for predicting fluid flow and heat transfer in separating and reattaching flows–II. Thermal field calculations, *Int. J. Heat. Mass. Tran*. 38 (8) (1994) 1467-1481.

[17] FLUENT 6.3 User's Guide.

[18] B. Yu, B. Q. Deng and C. N. Kim, Performance evaluation P-1 model in a photocatalytic reactor, *Chem. Eng. Sci*. 63 (2008) 5552-5558.

Chang Nyung Kim is a full professor of the Department of Mechanical Engineering, College of Engineering, Kyung Hee University in the Republic of Korea. His research focuses on computational fluid dynamics, micro-fluidic flow, heat transfer, biomechanics, and environmental fluid mechanics.